JOURNAL OF AIRCRAFT
Vol. 38, No. 4, July–August 2001

Three-Dimensional Gore Design Concept for High-Pressure Balloons

Nobuyuki Yajima,* Naoki Izutsu,† and Hideyuki Honda‡
The Institute of Space and Astronautical Science, Kanagawa 229-8510, Japan
Haruhisa Kurokawa§
Mechanical Engineering Laboratory, Ibaraki 305-8564, Japan
and
Kiyoho Matsushima¶
Fujikura Parachute Company, Tokyo 142-0063, Japan

A new design concept, named three-dimensional gore design, is investigated for the development of a large superpressure balloon capable of carrying a heavy payload. The theoretical and experimental studies are contrasted with the conventional natural shape balloon design. Each gore of the three-dimensional gore balloon has a bulge of small local radius between adjacent load tapes. This bulge is obtained not by film elongation but by adding excess film in both the circumferential and meridional directions. The longer edge of the gore is attached to the shorter load tape in a controlled shortening ratio. The film tension is zero in the meridian and extremely low in the circumferential direction in proportion to small local radius of a bulge. In addition, the maximum pressure of this balloon does not depend on the balloon volume. Test balloons of several sizes have been manufactured to confirm the feasibility of the three-dimensional design concept. Indoor full inflation tests and a flight test of these balloons have been performed successfully.

Introduction

AN essential research subject for a high-strength balloon is to improve balloon design so that film tension reduces under the same pressurized conditions. Reduction of film tension is achieved by making the radius of curvature of the film small. In this paper the authors propose a new balloon design concept, named three-dimensional gore design, where each gore forms a bulge of a small circumferential radius between adjacent load tapes without any film elongation. Such a gore shape is obtained by adding excessive film not only along the circumference but also along the meridian and by attaching the edge of the gore to the shorter load tape in a controlled shortening ratio. This three-dimensional gore design concept was introduced at the 32nd COSPAR Scientific Assembly.[1] The characteristics of this concept and experimental results of test balloons are described in detail in contrast with the conventional natural shape balloon.

The concept of natural shape, which is the basis of modern large balloon design, was originated by Upson[2] in 1938 and formulated by the University of Minnesota in the 1950s. In the early 1960s Smalley[3] calculated various balloon shapes under typical design parameters using a computer. These balloons do not have load tapes, and their axis-symmetrical shapes are derived under simple constraints, such as constant meridional length and infinitesimal excess along the circumference. The latter constraint is equivalent to the well-known condition that the circumferential tension is zero at an arbitrary point. This balloon shape is obtained by solving an equilibrium between pressure and film tension applied to a small segment on the balloon surface.

If the pressure at the base of the balloon is larger than ambient pressure, the shape of the balloon becomes that of a pressurized natural shape balloon. When the pressure is large, the shape is flattened and called a "pumpkin balloon." If the payload and film weight are negligible or the pressure is very large, the pumpkin becomes symmetric with respect to the equatorial plane (Euler's elastica). This original natural shape design concept does not consider film elongation. The balloon shape and film tension are derived independently of film extensibility as a statically determinate problem, owing to its unidirectional film tension.

At the apex and the base this natural shape balloon has singular points where the meridional tension becomes infinite. Modern large scientific balloons introduce a simple load-tape system constructed with fibers of high tensile strength and low extensibility. This system avoids the singular condition and increases payload capability significantly because the load tapes can transfer a concentrated payload weight to the balloon film smoothly. In addition, this load-tape system has a large potential for increasing balloon strength through the use of fiber reinforcement. The three-dimensional gore balloon design concept aims to enhance this effect up to its theoretical limit.

In the usual balloon manufacturing process load tapes are joined to the gores when their edges are sealed together. Because the spindle shape gore is made from flat film, the centerline length of the gore is shorter than the edge. A horizontal cross section of this balloon before film elongation is a polygon with load tapes at its corners. Hereafter this balloon is called a "flat-gore balloon." When this balloon is pressurized, the film expands outward between adjacent load tapes and forms bulges through film extensibility to sustain the load tapes. Because of this phenomenon, the flat-gore balloon has the following problems:

1) The meridional load is shared between load tapes and film. This sharing is counterproductive because the strong load tapes do not contribute to support all meridional tension.

2) The large circumferential gore radius results large circumferential tension on the film.

3) The statically determinate condition, which is the core idea behind the natural shape balloon to simplify its analysis, is spoiled.

All of these problems are caused by bidirectional film elongation.

Until now, many efforts have been made to analyze the shape and film tension distribution of the flat-gore balloon.[4,5] Those results show that the balloon shape and film tension also differ from those of the original natural shape balloon. Nevertheless, not only

Received 8 December 1999; revision received 20 June 2000; accepted for publication 8 February 2001.

*Professor, Scientific Ballooning Division. Member AIAA.
†Research Associate, Scientific Ballooning Division. Member AIAA.
‡Research Engineer, Engineering Support Division. Member AIAA.
§Senior Researcher, Head of Sound and Vibration Laboratory. Member AIAA.
¶Senior Engineer, R&D Division.

zero-pressure balloon but also superpressure balloon research has been based on the load-tape assembly of the flat-gore-balloon. For example, in early research on a pumpkin-type superpressure balloon with load tapes when Smalley proposed his e-balloon,[6] he suggested the superior effects of bulges of small radius. He, however, tried to achieve bulges through the effects of film extensibility. A similar attempt was also carried out by Rougeron,[7] Centre National d'Eludes Spatiales, in the 1970s.

In the flat-gore balloon the only design parameter is gore width as its length is fixed. Shur[8] analyzed the film tension distribution of pumpkin balloon under various modification of gore width. Excess film only in the circumference disturbs the uniformity of distribution of film tension. In some cases the total balloon strength is less than that of a sphere balloon.

The consequences of the disadvantages of the flat-gore design just mentioned are not so serious for a zero-pressure balloon with the good extensibility of the typical balloon films, such as Strato-E, SF372, or equivalent materials. The effects, however, become obstacles when we try to develop highly pressurized large balloons.

New Balloon Design Approach

Three-Dimensional Gore Design Concept

To avoid the problems of the flat-gore design approach just mentioned, we design a balloon such that each gore can form an ideal three-dimensional bulge without making use of film extensibility. For this purpose the gore has excess film along the meridian, and the width of the gore is the length of a circular arc. Then the meridional tension T_m becomes zero, and circumferential tension T_c is given by

$$T_c = P R_c \tag{1}$$

where P is the differential pressure and R_c is circumferential radius of bulges.

Like the original natural shape balloon without load tapes, the film tension is unidirectional, but the direction of tension is not along the meridian but along the circumference. With this condition on tension, a bulge with a small circumferential radius can be realized. In those conditions the circumferential radius R_c is a design parameter. When R_c is fixed at a certain value and film weight and the pressure gradient along a balloon height are negligible, the film tension is constant. In addition, the radius R_c does not depend on balloon volume. Because we usually make the maximum gore width equal to the effective width of the rolled film L_{fil}, the applicable minimum gore radius $R_{c,\min}$ is defined as

$$R_{c,\min} = L_{\text{fil}}/\pi \tag{2}$$

Thus the achievable minimum film tension $T_{\min}$ is

$$T_{\min} = P L_{\text{fil}}/\pi \tag{3}$$

This relation means that the burst pressure also does not depend on the balloon volume.

Figure 1 shows the balloon with an ideal gore shape, in which L_{load}, L_{meri}, and L_{arc} denote the length of the load tape, the meridional center line of the bulge, and the circumferential circular arc, respectively. As the gore is made of two-dimensional flat film, the cutting pattern of the gore is drawn so that its length is L_{meri} and width is L_{arc}. Here, L_{meri}, and L_{arc} are the same as those of the three-dimensional bulge, but the edge, which is joined to a load tape, is longer than the load tape. This longer edge should be attached to the shorter load tape by some method according to a certain shortening ratio K_s. This ratio is a function of the position along the meridian, that is, the ratio of the small segment on the load tape and that on the corresponding edge of the gore.

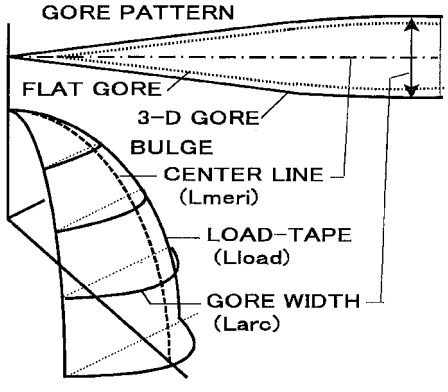

Fig. 1 Three-dimensional gore design concept.

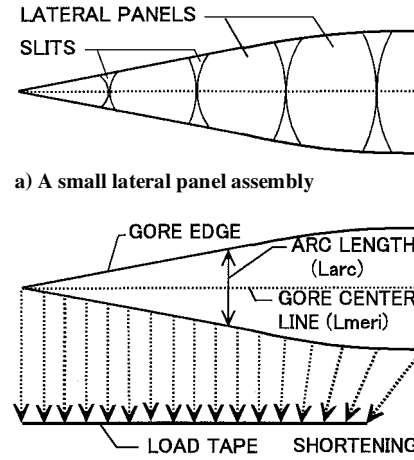

Fig. 2 Two fabrication methods for making bulges.

The design and analysis of the three-dimensional gore balloon is detailed in the Appendix. This design method is straightforward because it is based on the statically determinate problem like the original natural shape concept. With this characteristics the three-dimensional gore balloon is regarded as a family of a natural shape balloon.

How to Fit the Longer Gore to the Shorter Load Tape

This subject is the key point of the three-dimensional gore design concept. Some applicable methods can be found in dressmaking and tailoring technologies where well-fitting dresses and suits are made from flat cloth. There are two candidate techniques for making three-dimensional gore as shown in Figs. 2a and 2b:

1) Divide a long gore into small lateral panels that form a barrel shape. After these panels are joined to each other, the total edge length becomes the same as that of the load tape.

2) Join a long single sheet gore to the load tape with wrinkles, gathers, or tucks, according to the shortening coefficient *Ks*.

For large scientific balloons the first method is obviously not suitable because of extreme increase in the number of seals. The second method is acceptable if some new manufacturing methods are applicable for installation of load tapes. Possible shortening techniques are the following:

1) For polymer film, after gores are joined by heat seal or bonding with an auxiliary tapes, then the tapes are joined to load tapes with wrinkles.

2) For a fabric gore, sew with wrinkles, gathers, or tucks if applicable.

3) Gores are joined to prestretched load tapes. After pretension is released, gores have wrinkles. In this case the amount of stretch of the load tape caused by the pressure at the maximum altitude must be considered.

Experimental Results

Series of Pumpkin Balloon Models

Experimental research has been proceeding using different size model balloons as shown in Table 1. The gore material was a thin nylon fabric with urethane coating as a gas barrier and the load-tape material was the alamid fiber. The specifications of the fabric and the load tape are noted in the table.

Table 1 Specifications of the test balloons

Model no.	#1	#2	#3	#4	#4′
Volume, diameter	(1 m)	(3 m)	100 m^3	3000 m^3	3000 m^3
Film strength	——	10 kN/m	7 kN/m	7 kN/m	7 kN/m
Elongation	——	30%	30%	30%	30%
Bulge radius	——	0.5 m	0.8 m	0.8 m	0.8 m
Number of load tapes	8	12	18	55	55
Load tape stiffness	——	16 kN	16 kN	18 kN	18 kN
Maximum test pressure	——	187 hPa[a]	50 hPa[b]	10 hPa[c]	15 hPa[d]
Date	Jan. '98	Jun. '98	Feb. '99	March '99	May '99

[a]Actual burst pressure.
[b,c,d]Estimated burst pressure depended on the film strength is 88 hPa.
[c]Suspended as a result of the top part failure.

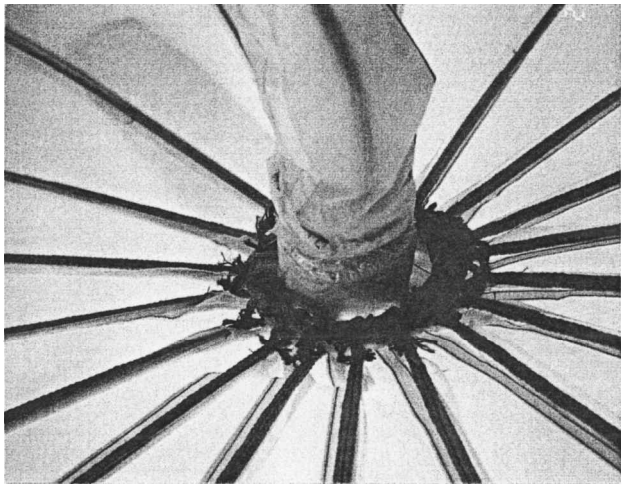

Fig. 3 Fitting for top and bottom of the balloon—conventional and three-dimensional gore designs.

As the first step, a small model 1 m in equatorial diameter was made in January 1998 to confirm the possibility of forming a large bulges of three-dimensional gore design (#1 in Table 1).

The second model was a balloon 3 m in equatorial diameter with 12 load tapes (#2 in Table 1). The gores were joined like a parachute using a sewing machine, and the seams were covered with hot melt seal tapes. Corresponding points on the load tapes and the joint lines of the gores were marked at intervals beforehand, and these pairs of points were aligned together in the assembly process. The designed bulge radius was 0.5 m, and the theoretical maximum pressure was 200 hPa.

A third model 100 m^3 in volume with 18 load tapes (#3 in Table 1) was manufactured for the verification of a new fabrication method that manages to fit the longer gore to the shorter load tape. The fitting process was accomplished continuously by means of the "gathering" function of a sewing machine. After the gores were seamed with each other and the seam lines were sealed, they were sewed to the load tapes with wrinkles. The computer-controlled sewing machine can make wrinkles with a variable density. The bulge radius was designed to be 0.8-m so that the maximum gore width was coincident with the effective film width of 1.35 m. With 0.8-m radius the theoretical burst pressure of the gore was 88 hPa. The load tapes were gathered at the top and bottom to fittings of metal rings of 20 cm in diameter as shown in Fig. 3.

Based on the successful test results of the preceding three balloons, the first flight model balloon 3000 m^3 in volume with 55 load tapes was manufactured in March 1999 (#4 and #5 in Table 1) as a scaled-up version of the 100-m^3 balloon.

Indoor Inflation Tests

A burst test of the 3-m balloon was carried out in June 1998. The balloon withstood up to 187 hPa, which was 3.4 times stronger

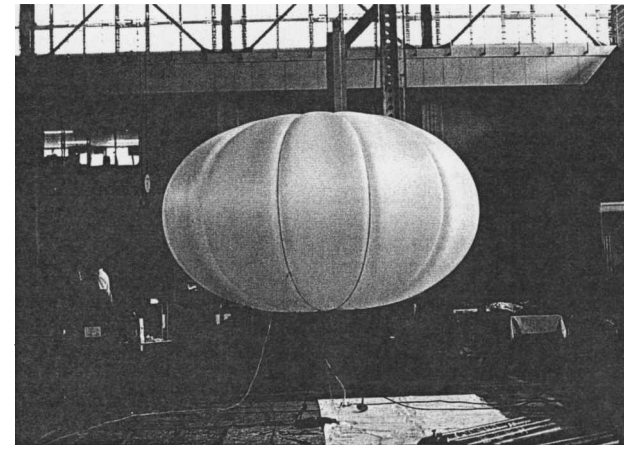

a)

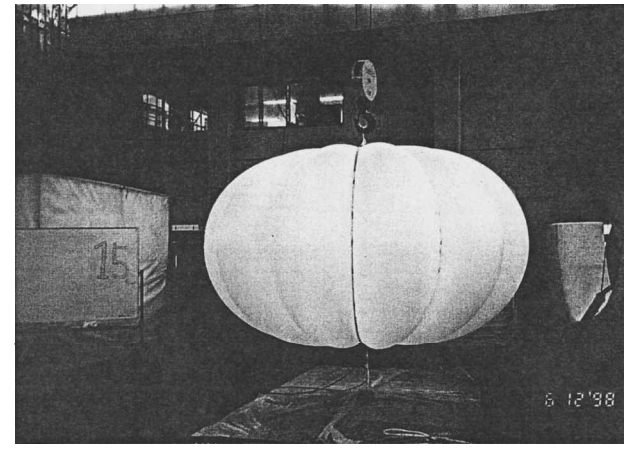

b)

Fig. 4 Comparison of the shapes of 3-m balloons of a) conventional and b) three-dimensional gore design.

than the same size flat gore balloon. Figure 4 shows the external appearance of two types of the same size balloon under low pressure. The balloon in Fig. 4a shows the flat-gore design, and the balloon in Fig. 4b uses the three-dimensional gore design. It is clear that the three-dimensional gore design balloon has lobed shape at this stage. The burst pressure also exceeded the similar size sphere balloon, which was tested as the first phase of NASA's ULDB program.[9]

An indoor full-inflation test of the 100-m^3 balloon was performed in February 1999 (Fig. 5). The three-dimensional gore shape achieved by the gathering sewing process was satisfactory. Though the balloon was not pressurized over 50 hPa for safety reasons, it appeared to have enough strength in reserve.

Prior to the actual flight, the 3000-m^3 balloon was also tested indoors twice in March and April 1999. The balloon was fully inflated

(Fig. 6), and its pressurized behavior was carefully observed. In the first test there was a short split in the film near apex when pressure reached 10 hPa because of the lack of the circumferential fullness. For the second test the balloon was pressurized to 15 hPa successfully and also appeared to have enough strength in reserve.

We directly measured the bulge radius by fitting concave patterns to the gore surface. As shown in Figs. 7a–7c, at the beginning of pressurization, the radius of each balloon was larger than its designed value, but it converged to the designed value as the pressure increased. This deviation of the bulge shape from the designed one at the low pressure was caused by the relatively large effects of compression force and bending moment of the wrinkles.

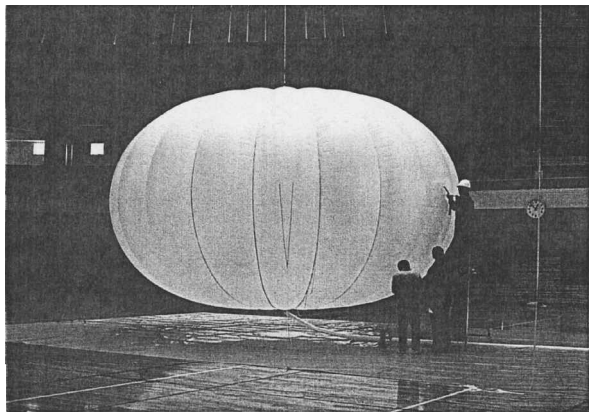

Fig. 5 Inflation test of a 100-m^3 balloon.

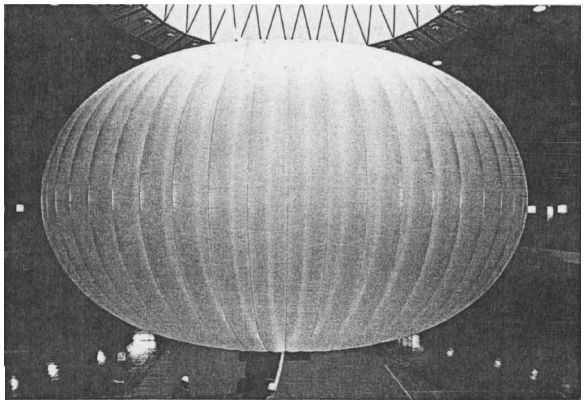

Fig. 6 Inflation test of a 3000-m^3 balloon.

Film strain was also measured by observing the stretched length of two reference lines drawn on the gore surface orthogonally. Because film elongation was not counted in the gore design, the meridional strain occurred as the circumferential elongation increased. This meridional strain was smaller than the circumferential strain, and the pressure was supported mainly by the circumferential tension because the former radius of curvature is larger.

As shown in Fig. 8, the circumferential strain was about 20% at the burst pressure of 187 hPa in the 3-m balloon. Expected burst pressure of 85 hPa for the 100-m^3 balloon and 40–60 hPa for the 3000-m^3 balloon were extrapolated from the strain data (dotted lines in Fig. 8), although the latter estimation has large uncertainty because of limited data points. These maximum pressures appear to be consistent with the theoretical pressure derived from film strength and circumferential bulge radius. These experimental results substantiate the theoretical prediction that burst pressure does not depend on the balloon volume.

Flight Test

A flight test of the 3000-m^3 superpressure balloon was performed in May 1999. The specifications of this flight test are listed in Table 2. The profiles of the balloon altitude and pressurized state are shown in Fig. 9. The balloon stopped ascending at an altitude of 19 km under a pressure difference of 13 hPa. At this pressure 6.5 hPa is derived from the product of the free lift rate (10%) and the ambient pressure of 65 hPa. The remaining component of the pressure of 6.5 hPa is caused by the heat-up effect caused by the solar radiation. From the meteorological data the ambient temperature at the altitude of

Table 2 Specifications of the fight test of the 3000 m^3 balloon

Item	Weight (kg)
Balloon	151
Payload	36
Ballast	90
Rigging	11
Total	288
Free lift	35

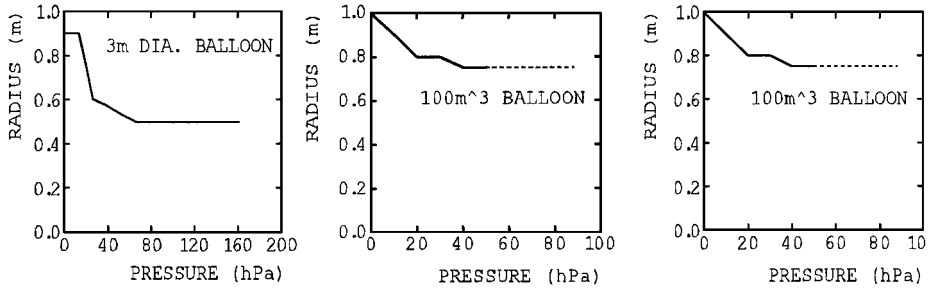

Fig. 7 Circumferential bulge radius.

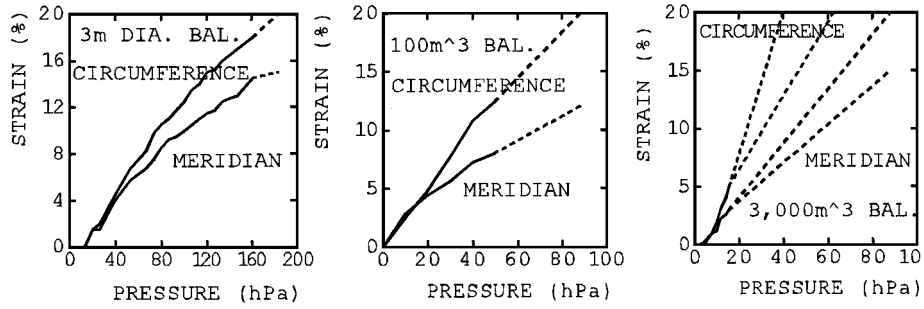

Fig. 8 Film strain vs pressure.

19 km was 216 K. Therefore, the pressure of 6.5 hPa corresponds to the fact that the temperature of the buoyant gas is 18 K higher than that of the ambient atmosphere.

We then dropped ballast repeatedly and increased balloon pressure in order to verify the strength of the balloon. When all 90 kg of ballast were consumed, the balloon reached the altitude of 21 km, and the pressure difference increased to 29 hPa, which was 63% of the ambient pressure (46 hPa). At this moment the total meridional tension supported by 55 load tapes was about 1000 kN, resulting in 18.2 kN per load tape, which value exceeded the ultimate strength of the 18-kN Kevlar rope. The flight ended when one of the load tapes broke.

Figure 10 shows the shape of the balloon looking upward from an onboard camera attached to the payload. In this picture we can see that the film forms large bulges between load tapes. Because the straight-line distance between adjacent load tapes is known, the bulge radius of 0.8 m is estimated from this picture. This radius is almost the same as the designed value.

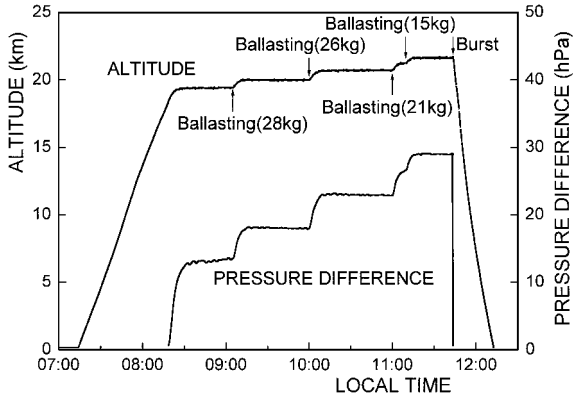

Fig. 9 Profile of flight altitude and differential pressure.

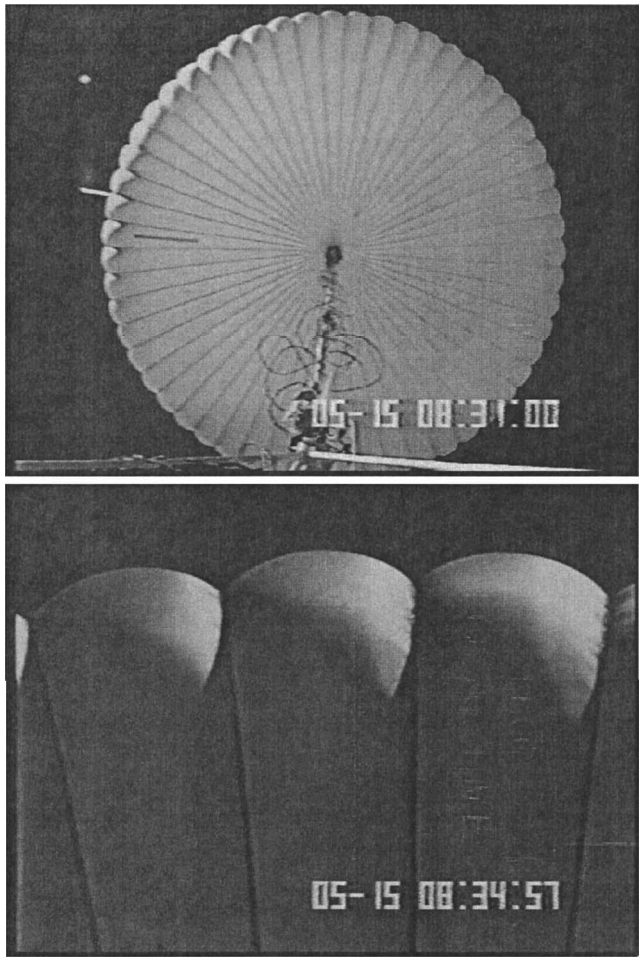

Fig. 10 Shape of the balloon seen from an upward-looking camera.

Conclusions

We can obtain extra strength balloons by applying the three-dimensional gore design concept using the strong films developed by current research. This concept was verified through the indoor inflation tests and flight test. The burst pressure for the three-dimensional gore balloon will exceed the pressure levels required for typical stratospheric superpressure balloons, even if the balloon volume is quite large. For instance, if the film strength is 10 kN/m and the designed circumferential radius is to be 1 m the burst pressure is estimated to be 100 hPa. If the actual pressurized level is 10% of ambient pressure, it is 6, 1, and 0.6 hpa at 20, 30, and 35 km in balloon altitude, respectively. The burst pressure of 100 hPa still exceeds the required level even if a safety factor of 10 is adopted.

On the other hand, the disadvantage of the strong films is their heavy unit weight, which is three to five times that of conventional thin polyethylene film. Thus there are two main strategies for the future advancement of super-pressure balloon technologies:

1) Develop medium-strength film (about 2–5 kN/m) as light in weight as conventional polyethylene balloon film.

2) Use strong film, but make full use of the extra-strong characteristics of the three-dimensional gore balloon. For instance, use a combination of the two kinds of balloons: a zero-pressure balloon supporting the payload and a superpressure balloon controlling buoyancy.

Development of medium-strength film belongs to the field of material science. As for two-balloon combinations, candidates are a double-capsule balloon, which installs a relatively small superpressure balloon inside a large zero-pressure balloon, and a tandem balloon, which is the revival of the "Sky Anchor" balloon system investigated in the 1970s. The pressurized level of the small superpressure balloon increases in proportion to the volume ratio of two balloons because the superpressure balloon must suppress not only the free lift of itself but also that of the zero-pressure balloon. The volume ratio of about 1 : 5 is normally selected. The three-dimensional gore design balloon is strong enough to withstand such a high pressure. The advantage of this system is that the total weight of two balloons is obviously lighter than a single superpressure balloon with the same volume.

Appendix: Formulation of Three-Dimensional Gore Design

Nomenclature

l	=	length along gore centerline
N	=	number of gores = number of load tapes
p	=	gas pressure difference
R_c	=	minimum radius of curvature of bulge surface
R_m	=	radius of curvature of load tape
s	=	length along load tape
$\boldsymbol{T}$	=	film tension vector
T_L	=	load tape-tension
X	=	coordinate variable along axis of symmetry
x axis	=	tangent to load tape
Y	=	coordinate variable of load tape, distance from axis of symmetry
z axis	=	normal to plane tangent to two adjacent load tapes
α	=	half of angle between local tangent lines to two adjacent load tapes
β	=	half of arc angle of bulge curve
θ_c	=	angle of z axis to horizontal plane
θ_m	=	angle of normal vector of load tape to horizontal plane
ϕ	=	angle of z axis to normal plane of bulge surface
φ	=	angle between z axis and the normal to load tape

Here our three-dimensional gore design is outlined. First, let us consider a smoothly curved surface bulging outside between two load tapes as shown in Fig. A1. It is assumed that the film tension is unidirectional along the circumferential direction at any point, that

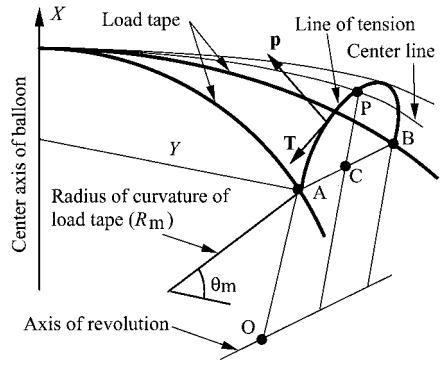

Fig. A1 Film surface and line of tension.

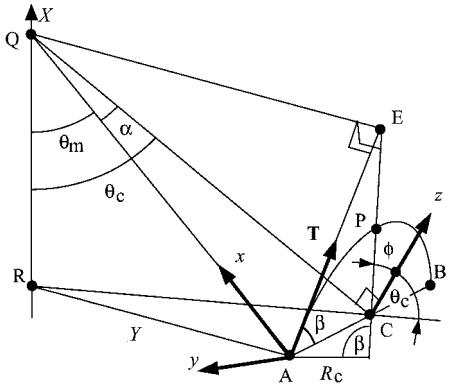

Fig. A2 Direction of surface tension.

is, the film has infinitesimal excess in the meridional direction. By tracing the direction of tension $\boldsymbol{T}$, curved lines connecting adjacent load tapes are obtained as APB in Fig. A1. Each line, called the line of tension hereafter, lies on a plane, and the surface is locally perpendicular to this plane hence it is locally a surface of revolution. For this surface of revolution, the force balance between the tension and gas pressure for each small segment is maintained the same as in the natural shape balloon even though the axis of revolution is horizontal in this case. Though the line of tension is not a circular arc, it can be regarded so if the number of the load tapes, denoted by N, is large enough. (In Fig. A1 the radius of revolution OA and its difference PC in maximum can be evaluated by R_m and AC, respectively. When N is large, AC is much smaller than R_m. As the tension of the natural shape balloon (Euler's elasltica) is inversely proportional to the radius of revolution, it is almost constant in this case, hence the line of tension is a circular arc.) In this case the radius of the circular arcs is regarded the same everywhere, which is denoted by R_c.

Let us describe the shapes of the film surface and the load tape considering balance of force acting on the load tape. In Fig. A1 the load tape is described by the coordinates (X, Y) and also by (R_m, θ_m). In the following gas pressure denoted by p is considered large and set constant. Also, the weights of the film and the load tapes are neglected, while they are easily included in the equations.

Let us define local coordinates and several angles. In Fig. A2 the point Q is the intersection of the load tape's tangent at A and X axis. Local coordinates are set with x axis tangent to the load tape, z axis normal to the plane ADB in Fig. A2, and y axis forming a right-handed coordinate system. The angles θ_c and ϕ are angles between z axis and the horizontal line (RC) and between z axis and CP, respectively. They are given by

$$\tan\theta_c = \tan\theta_m \sin(\pi/N) \tag{A1}$$

$$\sin\phi = \tan\alpha \tan\beta \tag{A2}$$

where α and β are defined in Fig. A2 and given by

$$\sin\alpha = \sin\theta_m \sin(\pi/N) \qquad \sin\beta = Y \sin(\pi/N)/R_c \tag{A3}$$

Equation (A2) is derived from the fact that the line AQ and the tension vector $\boldsymbol{T}$ are both tangent to the film surface at A; hence, QE is perpendicular to CP in Fig. A2.

With gas pressure p the film tension vector $\boldsymbol{T}$ at A expressed in the local coordinates is given as

$$\boldsymbol{T} = (T_x, T_y, T_z) = R_c p(\sin\alpha/\cos\beta, \sin\alpha\sin\beta\sin\phi - \cos\alpha\cos\beta, \sin\beta\cos\phi) \tag{A4}$$

The curvature of the load tape and the change in its tension are derived from the film tension of two adjacent films acting on the load tape's segment at A as

$$T_L/R_m = 2\cos\alpha\cos\phi(T_z\cos\varphi + F_y\sin\varphi) \tag{A5}$$

$$\mathrm{d}T_L = -2\,\mathrm{d}s\cos\alpha\cos\phi T_x \tag{A6}$$

Here, T_L denotes the load-tape tension and $\mathrm{d}s$ $(=\mathrm{d}\theta_m R_m)$ denotes the small segment length of the load tape. Angle φ denotes the angle between z axis and the normal to the load tape (z' in Fig. A3). It is given by

$$\sin\varphi = \cos\theta_m\cos\theta_c\cos(\pi/N) + \sin\theta_m\sin\theta_c \tag{A7}$$

The differential $\mathrm{d}l$ of the gore center line length l follows:

$$\mathrm{d}l = \mathrm{d}s\cos\alpha\cos\phi + R_c(1-\cos\beta)(\mathrm{d}\phi + \mathrm{d}\theta_c) \tag{A8}$$

because the film segment APBB′P′A′ in Fig. A3 is locally a torus. Here, $\mathrm{d}\phi$ and $\mathrm{d}\theta_c$ are expressed by $\mathrm{d}\theta_m$ using differentials of Eqs. (A1–A3).

By substituting Eq. (A4) into Eq. (A5), R_m is obtained. Using this, the shape of the load tape given by (X, Y) is described by differential equations of θ_m. By the numerical integration of these as well as Eqs. (A6) and (A8) with appropriate initial values of T_L and Y, the load-tape shape, the centerline length of the gore, the film width $2R_c\beta$, and the load-tape tension are obtained as functions of θ_m. In the actual calculation the initial values are determined by several integrations to satisfy the condition of the final values. At the same time the shortening ratio K_s (see Fig. 2) defined by

$$Ks = \frac{\mathrm{d}s}{\sqrt{(R_c\,\mathrm{d}\beta)^2 + \mathrm{d}l^2}} - 1 \tag{A9}$$

is obtained to fit a flat film to the defined curved surface.

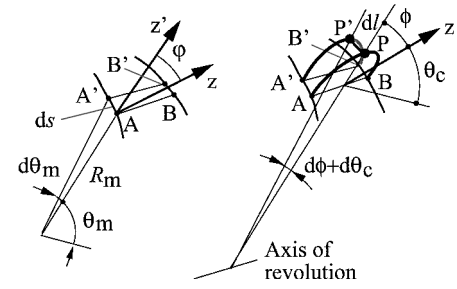

Fig. A3 Differentials.

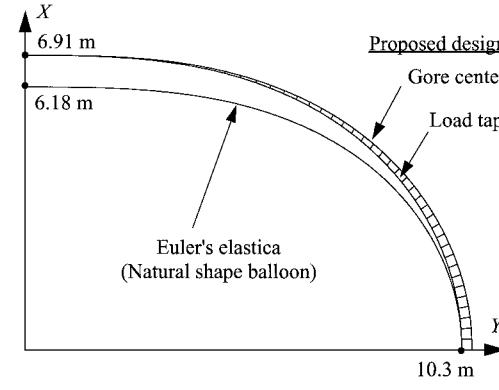

Fig. A4 Results of calculation.

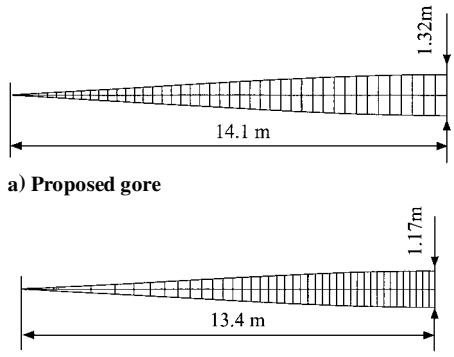

Fig. A5 Half of gore shape. (Vertical lines correspond to lines of tension for several θ_m with constant difference.)

The preceding discussion is formulated as a statically determinate problem where the film tension is unidirectional. Once the three-dimensional shape is obtained, film deformation can be evaluated easily for given Young's modulo and Poisson's ratio, hence can be included in the design. As the tension along the circumferential direction is constant and that along the meridional direction is zero, the width and the length of the gore before tension is applied should be made small and large respectively by the constant ratios. The elongation of the load tapes can be also evaluated separately. Thus this design is straightforward compared with other designs that need optimization among various gore designs with respect to two-dimensional deformation analysis of the film by using further approximation or by finite element method.

Figures A4 and A5 show results of calculation where $N = 55$, $Y_{\max} = 10.3$ m, and $R_c = 0.8$ m as is the case of model #4 of the experiments. The shortening ratio of the film edge is 4.6% in maximum. At $p = 10$ hPa the film tension T is 800 N/m, and the maximum tension of one load tape is 6260 N.

Acknowledgments

The authors would like to express many thanks to Motoki Hinada for his kind encouragement to our research activity. This research was supported financially in part by the Japan Science and Technology Corporation.

References

[1] Yajima, N., "A New Design Approach for Pressurized Balloon," *Advanced Space Research*, Vol. 26, No. 9, 2000, pp. 1357–1360.

[2] Upson, R. H., "Stresses in a Partially Inflated Free Balloon—with Notes on Optimum Design and Performance for Stratosphere Exploration," *Journal of Astronautical Science*, Vol. 6, No. 2, 1939, pp. 153–156.

[3] Smalley, J. H., "Determination of the Shape of a Free Balloon," Air Force Cambridge Research Laboratories, AFCRL-65-92, Bedford, MA, Feb. 1965.

[4] Alexander, H., and Agrawal, P., "The Effect of Material Deformation on the Shape and Stress State of a High Altitude Balloon," *7th AFCRL Scientific Balloon Symposium*, Air Force Cambridge Research Laboratories, AFCRL-TR-73-0071, Special Rept. 152, Bedford, MA, pp. 397–414.

[5] Schur, W. W., "Structural Behavior of Scientific Balloons; Finite Element Simulation and Verification," *AIAA International Balloon Technology Conference*, AIAA, Washington, DC, 1991, pp. 89–93.

[6] Smalley, J. H., "Development of the e-Balloon," *Proceedings of 6th AFCRL Scientific Balloon Symposium*, Air Force Cambridge Research Laboratories, AFCRL-70-0543, Special Rept. 105, Bedford, MA, 1970, pp. 167–176.

[7] Rougeron, M., "Up to Date CNES Balloon Studies," *Proceedings of 10th AFCRL Scientific Balloon Symposium*, Air Force Geophysics Laboratory, AFGL-TR-79-0053, Special Rept. 217, Hanscom AFB, MA, 1978, pp. 39–57.

[8] Schur, W. W., "Structural Analyses of Balloons Employing Techniques to Overcome Difficulties Posed by the Underconstrained Nature of These System," AIAA Paper 96-0577, 1996.

[9] Smith, M. S., Seely, L. G., and Stephen, R. S., "Current Status of Advanced Materials and Seaming Research," *Proceedings of the 21st International Symposium on Space Technology and Science*, Vol. 2, 1998, pp. 1614–1620.